Int. J. Solids Structures, 1966, Vol. 2, pp. 555 to 571. Pergamon Press Ltd. Printed in Great Britain

SECOND-ORDER VISCO-ELASTICITY IN A FILLED ELASTOMER

B. ALBRECHT and A. M. FREUDENTHAL

Columbia University, New York

Abstract—The mechanical behavior of polyurethane rubber filled with granular potassium chloride was investigated by subjecting tubular specimens to oscillatory torsion. The response of the material was studied to variation of frequency and amplitude of the imposed strain as well as to variation of the temperature.

Beside the measurement of the storage and loss moduli the normal forces are observed and the second-order moduli of cross-elasticity, cross-viscosity and cross-visco-elasticity are evaluated.

INTRODUCTION

CHARACTERIZATION of the mechanical response of highly filled elastomers is usually based on the results of creep or relaxation tests combined with those of free transient or resonant stationary oscillations of small amplitudes, evaluated on the basis of the assumptions defining linear visco-elastic thermo-rheologically simple media. In the present investigation an attempt is made to use for this purpose forced cyclic shear with controlled moderate strain amplitudes under such experimental conditions that not only the two first-order parameters (storage and loss moduli) of the linear response but also three additional second-order parameters resulting from the tensorial non-linearity could be recorded and evaluated. The validity of the concept of the simple temperature shift was also explored and the temperature-dependence of the second-order parameters established over a moderate temperature range. The visco-elasticity of the second-order response accompanying the visco-elastic response in shear was clearly demonstrated.

The material used was an inert model of a solid propellant consisting of polyurethane rubber filled with granular potassium chloride which has mechanical properties similar to those of the oxidizer of the live propellant; it was supplied by Aerojet General. The filler is made up of about 47% potassium chloride and 6% aluminum powder by volume. Microscopic examination of a freshly cut surface indicates the size of aluminum particles to be below 40 μ, while the potassium chloride particles range up to 200–300 μ. The predominant particle size appears to be of the order of 100 μ.

A previous study of the same material under conditions of creep and relaxation had shown [1] that the propellant behaves as a linear visco-elastic medium in the range of uniaxial strains up to 4 per cent and in shear up to 8 per cent and that the bulk modulus is of the order of 5×10^5 psi while Young's modulus at room temperature is below 10^3 psi, and varies only slowly with the strain rate. Thus it appeared reasonable to assume incompressibility of the material in this investigation.

1. SPECIMENS AND INSTRUMENTATION

The experiments were performed on the Weissenberg Rheogoniometer [2] from which

the cone and platten were removed to accept the circular plate holders of the specimens of the dummy propellant.

There were several considerations influencing the size and production technique of the specimens. Because of the high concentricity required, the tubular specimens were made by cementing carefully machined circular holders to a slab of the material ground to uniform thickness. After the cement was set, the specimens were cut out on a band saw, leaving substantial margins around the holders for further machining. These specimen blanks were then hollowed out on a lathe to the required inner diameter and the upper holders were then cemented concentrically to the free ends using reamed holes and mandrils for guidance. Finally, the whole unit mounted on the mandril was inserted between centers of a lathe and the outer surface properly finished.

The dimensions of the specimens, o.d. = 2·125 in. and i.d. = 1·875 in. were determined experimentally. On the one hand, the size of the filler particles required a minimum thickness, to allow the assumption of a homogeneous continuum and to diminish the effect of surface defects caused by the breaking and ripping out of filler particles in machining the specimens. On the other hand, the wall thickness had to be small in relation to the radius to permit the assumption of a uniform stress distribution, but sufficiently large to prevent local instability. With the dimensions as chosen the height of the specimen could be varied from 0·250 in. to about 2·00 in. For this part of the investigation, however, a height of 0·50 in. was used.

The Rheogoniometer as used is schematically shown in Fig. 1. Its basic parts are two plattens A and B. The upper platten A is fixed through a torque bar to a slide and thus

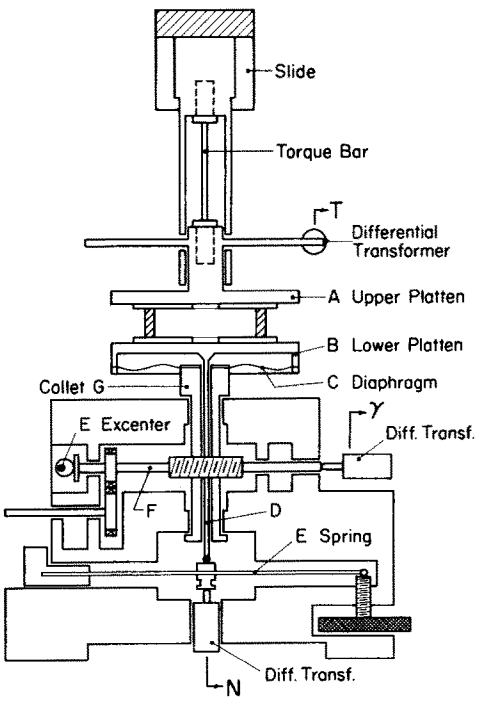

FIG. 1. Weissenberg Rheogoniometer.

to the frame of the machine. The twist of the torque bar, which is proportional to the applied torque, is picked up by a differential transformer T and the signal fed into one channel of a double channel x–y recorder. The whole slide assembly can be moved up and down and the distance between the two plattens can thus be arbitrarily set.

The lower platten B can either be rotated at a uniform rate, being driven through a worm on the shaft F and a gear attached to the collet G, or given an oscillatory motion of variable amplitude by translationary motion of the shaft F imparted to it by a rotating excenter E, or both motions can be combined. Both the rate of uniform rotation and the frequency of the oscillatory motion can be varied in small steps over a wide range by gear box controls.

As the lower platten is connected to the driven collet G by a special diaphragm C, the platten, although rigidly attached in rotational motion, can move within certain limits in the vertical direction. This motion, however, is resisted by a vertical rod D bearing on a flat spring H. By a proper choice of spring stiffness, the deflection of the spring can be kept fairly small (approx. 10^{-5} in.); it is measured by the differential transformer N. The transformer output is then amplified and fed into the second channel of the recorder.

For the oscillatory mode of operation the deformation of the sample is determined from the translationary motion of the driving shaft F. Its momentary position is sensed by the differential transformer R and its output fed into the x channel of the recorder.

The specimen assembly, including the lower and upper platten of the machine, can be enclosed by a chamber through which cooled or warmed air can be circulated, and thus the specimen can be brought to a desired test temperature.

2. TEST RESULTS

The oscillatory mode of operation of the Rheogoniometer appears most suitable for this investigation as the dynamic response of the propellant could be studied as a function of frequency and the linearity of the response could be easily checked by variation of the amplitude of the imposed deformation, as shown in Fig. 6. For clarity of diagrams, only two amplitudes are used.

The use of specimens of standard dimensions allowed calibration of the instrument in terms of stress and strain and thus stress–strain curves could be directly obtained for the various test conditions. In evaluating these diagrams, however, corrections are necessary as the indicated values contain also contributions from the deformation of the instrument. The nominal shear strain includes also the twist of the torque bar and the normal force is decreased because of the deflection of the spring resisting it.

The twist of the torque bar is proportional to the torque induced in the specimen and the correct strain is obtained by subtracting the strain due to this twist. This can be easily done in the recorded stress–strain diagrams by rotating the stress axis by a proper angle α, and then using the skewed axes as a basis for evaluation of the moduli, as shown in Fig. 2.

The correction for the deflection of the spring measuring the normal force can be made by repeating the measurements with a spring of a different stiffness and then evaluating the normal stress by extrapolation to zero deflection. Or the stress from a single spring measurement is corrected by the additional stress needed to push the specimen to zero extension. This additional stress is proportional to the compression

modulus and thus its values have to be known for all the test conditions. In both cases it is desirable to keep the deflection of the spring as low as possible as this results in more accurate initial values. Deflections of the order of 10^{-5} appear to be a practical limit, as with further decrease, the imperfections of the contact surfaces and the temperature effects constitute an appreciable portion of the measured deflection. The temperature effects especially proved to be troublesome in the present investigation. Improvement is necessary in the temperature control and the steel rod transferring the normal force to the spring has to be replaced by one made of invar, as a temperature change of 0·5°C results in change of length of the same order of magnitude as the measured deflection.

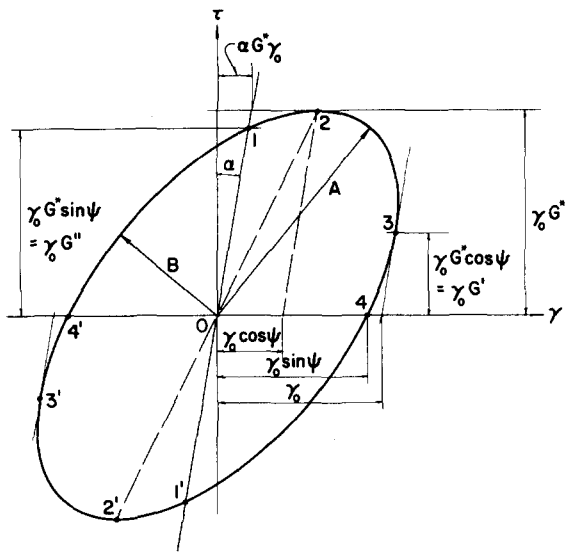

$$G' = \frac{\gamma_0 G^* \cos\psi}{\gamma_0} = G^* \cos\psi$$

$$G'' = \frac{\gamma_0 G^* \sin\psi}{\gamma_0} = G^* \sin\psi$$

$$\tan\psi = \frac{\gamma_0 \sin\psi}{\gamma_0 \cos\psi}$$

$$Wd = \pi \gamma_0^2 G^* \sin\psi = \pi AB$$

FIG. 2. Evaluation of storage and loss moduli from a typical shear stress–strain diagram in reversed torsion.

Some of the recorded stress–strain diagrams corrected for the normal force spring deflection and showing the correction angle α are shown in Fig. 3 through Fig. 7. From these diagrams and from diagrams not shown the values of the storage modulus and of the loss modulus in shear were evaluated and are presented as functions of $\log 1/\omega$ in Fig. 8. For comparison, a relaxation modulus in shear at room temperature obtained in a previous investigation is also shown in this diagram.

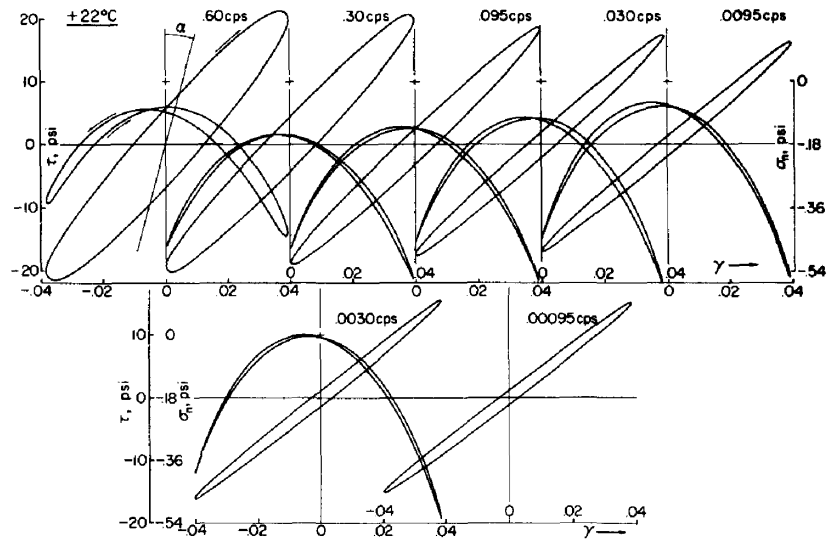

FIG. 3. Recorded shear stress–strain and normal stress–shear strain diagrams in reversed torsion at +22°C.

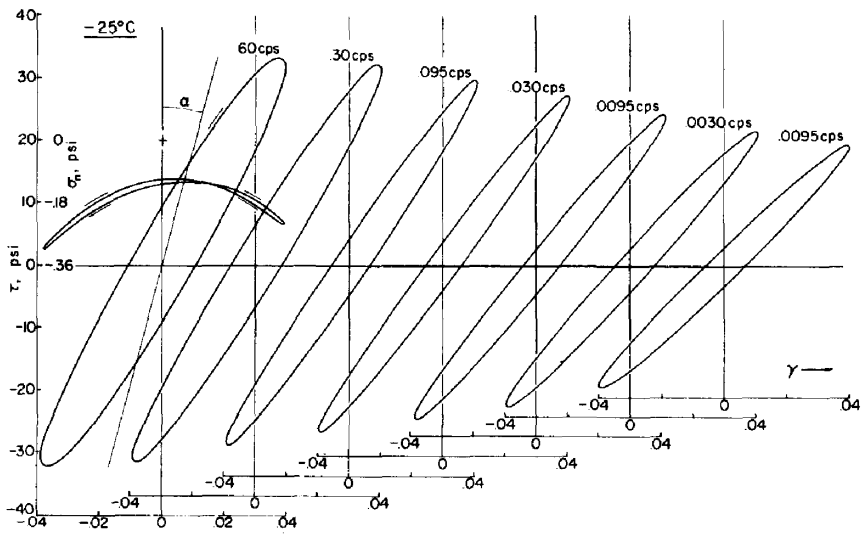

FIG. 4. Recorded shear stress–strain diagrams in reversed torsion at −25°C.

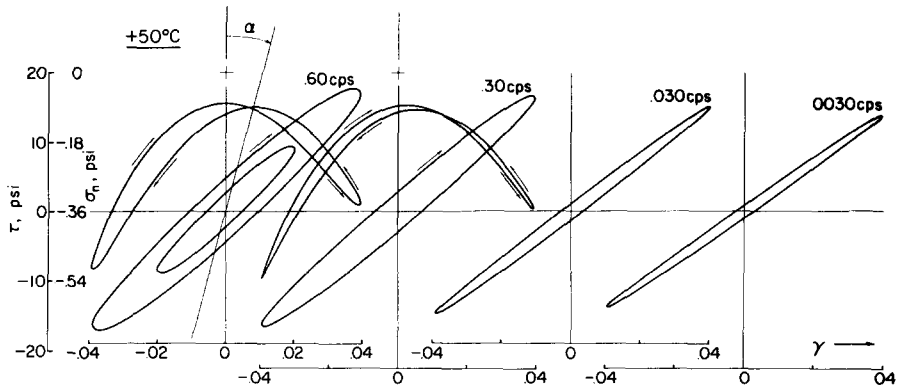

FIG. 5. Recorded shear stress–strain and normal stress–shear strain diagrams in reversed torsion at +50°C.

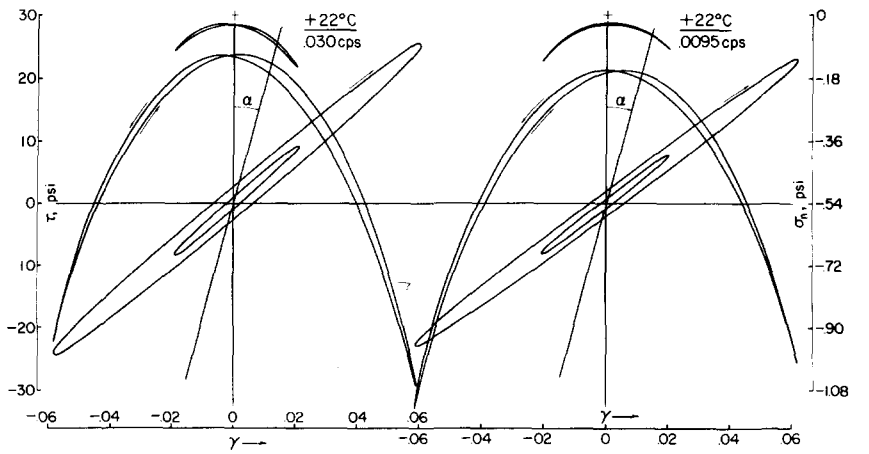

FIG. 6. Recorded shear stress–strain and normal stress–shear strain diagrams in reversed torsion for two amplitudes of the imposed cyclic strain at +22°C.

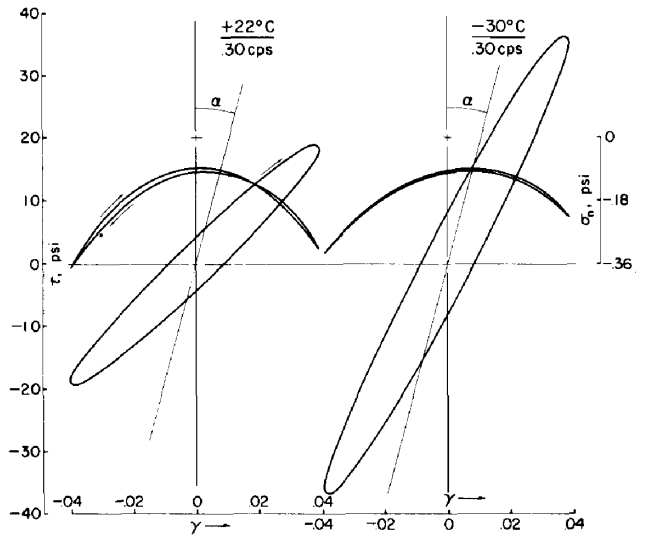

FIG. 7. Recorded shear stress–strain and normal stress–shear strain diagrams in reversed torsion at +22°C and −30°C.

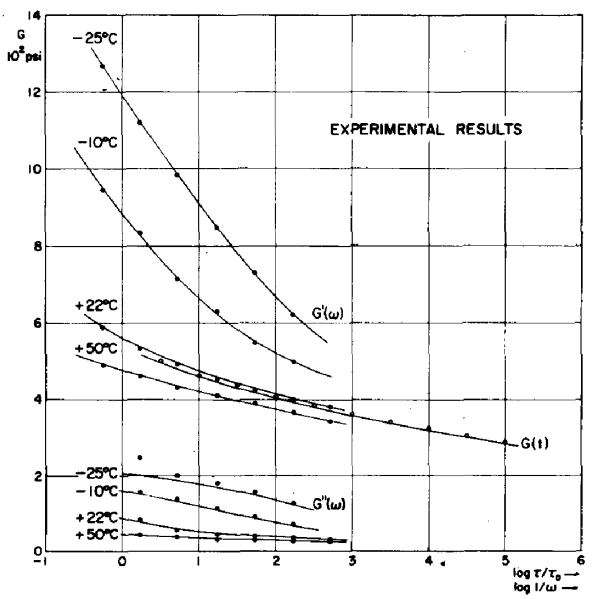

FIG. 8. Measured storage and loss moduli as functions of log $1/\omega$.

3. INTERPRETATION OF TEST RESULTS

As the propellant behaved in shear as an incompressible linear visco-elastic medium in the range of the test conditions, the interpretation of the test results was based on linear visco-elastic analysis.

Under zero initial conditions, the constitutive equations in the deviatoric form are given by equation

$$s_{ij}(t) = \int_0^t 2G(t-u)\frac{de_{ij}(u)}{du}\,du \tag{1}$$

where

$$G(t) = \int_0^w \frac{dG}{d\tau}\exp(-t/\tau)\,d\tau \tag{2}$$

is the relaxation modulus in shear, τ the relaxation time, $(t-u)$ the elapsed time, and $dG/d\tau = f(\tau)$ the intensity of the relaxation spectrum.

Equation (1) solved for the imposed oscillatory motion $2e_{12} = \gamma_0 \sin \omega t$ gives

$$s_{12}(t) = \gamma_0\left\{\sin\omega t\int_0^\infty \frac{\omega^2\tau^2}{1+\omega^2\tau^2}\frac{dG}{d\tau}\,d\tau + \cos\omega t\int_0^\infty \frac{\omega\tau}{1+\omega^2\tau^2}\frac{dG}{d\tau}\,d\tau\right.$$

$$\left. -\int_0^\infty \frac{\omega\tau}{1+\omega^2\tau^2}\frac{dG}{d\tau}\exp(-t/\tau)\,d\tau\right\} \tag{3}$$

where

$$G'(\omega) = \int_0^\infty \frac{\omega^2\tau^2}{1+\omega^2\tau^2}\frac{dG}{d\tau}\,d\tau \tag{4}$$

and

$$G''(\omega) = \int_0^\infty \frac{\omega\tau}{1+\omega^2\tau^2}\frac{dG}{d\tau}\,d\tau \tag{5}$$

are the storage and loss moduli in shear, respectively, and are the measurable quantities.

Because of the wide range of the function $f(\tau) = dG/d\tau$ the alternate expressions containing the intensity of the relaxation spectrum as a function of $\ln\tau$ are more often used; thus

$$G(t) = \int_{-\infty}^\infty H(\ln\tau)\exp(-t/\tau)\,d\ln\tau \tag{6}$$

$$G'(\omega) = \int_{-\infty}^{\infty} \frac{\omega^2\tau^2}{1+\omega^2\tau^2} H(\ln\tau)\, \mathrm{d}\ln\tau \tag{7}$$

$$G''(\omega) = \int_{-\infty}^{\infty} \frac{\omega\tau}{1+\omega^2\tau^2} H(\ln\tau)\, \mathrm{d}\ln\tau. \tag{8}$$

The intensity of the relaxation spectrum $H(\ln\tau)$ can in principle be determined from any of the three equations relating it to the measured quantities $G(t)$, $G'(\omega)$ or $G''(\omega)$, but in this investigation the approximation method of Alfrey as described by Leaderman [3] using equation (7) appeared to be most suitable.

Substitution of $\omega = \exp(-n)$ and $\tau = \exp(z)$ into equation (7) leads to

$$g'(n) = \int_{-\infty}^{\infty} H(z) \frac{1}{1+\exp[2(n-z)]}\, \mathrm{d}z \tag{9}$$

where $g'(n)$ is the storage modulus expressed as a function of $\ln 1/\omega$.

The rate of change of $g'(n)$ with respect to n is

$$\frac{\mathrm{d}g'(n)}{\mathrm{d}n} = -\int_{-\infty}^{\infty} H(z) \frac{2\exp[2(n-z)]}{\{1+\exp[2(n-z)]\}^2}\, \mathrm{d}z \tag{10}$$

and as for a given value of n the function multiplying $H(z)$ in the integrand has a rather limited range, and if $H(z)$ is a slowly varying function in this range, $H(z)$ can be replaced by a constant $H(n)$ and the integration easily performed. Equation (10) then becomes

$$\frac{\mathrm{d}g'(n)}{\mathrm{d}n} = -H(n). \tag{11}$$

The intensity of the relaxation spectrum is equal to the negative slope of the storage modulus when both are plotted as functions of $\ln 1/\omega$.

In a similar fashion, the equation

$$\frac{\mathrm{d}g(m)}{\mathrm{d}m} = -H(m) \tag{11a}$$

is obtained, where the intensity of the relaxation spectrum is related to the rate of change of the relaxation modulus in shear, when both are plotted as functions of $\ln\tau$.

If either the storage modulus or relaxation modulus were known over the whole range of the relaxation spectrum, the relaxation spectrum would be determined by the evaluation of the derivative of either of the moduli curves. The time range of the observed quantities, however, is limited by the experimental technique used and even a combination of several techniques does not, generally, give a complete coverage. More often only one or two experimental techniques are employed and the range is extended by variation of temperature and by connection of the "reduced" segments covering the limited time range of observation into a master curve using one of the time–temperature relations. Implicit in this time–temperature superposition is the assumption that all the relaxation or retardation mechanisms have the same time–temperature dependence, which in a case of a wide distribution of relaxation time does not appear to be reasonable.

4. TEMPERATURE SHIFT

If the experimental results presented in Fig. 8 are reduced to any reference temperature, the resulting curves cannot be shifted into a complete coincidence over the whole region of overlap, indicating that there is also a change of shape associated with the temperature change. Thus the possibility of the variation of the time–temperature relationship, even over the limited portions of the relaxation spectrum, must be admitted. In view of this, the concept of the simple spectrum shift on the logarithmic time scale [4] evaluated from the Arrhenius equation, and the Williams, Landel, Ferry [5] time–temperature relation are re-examined and modified.

Denoting $\tau/\tau_0]_{T_R} = \kappa$ and $\tau/\tau_0]_T = \lambda$, where τ_0 is an arbitrarily chosen unit of relaxation time scale, T is the Kelvin temperature and T_R the reference temperature, Alfrey's relation [6] can be written as

$$\ln \lambda = \ln \kappa + Q/R(1/T - 1/T_R) \tag{12}$$

where Q is the activation energy and R the gas constant. By replacing Q/R by a function $U(\ln \kappa)$ the time–temperature relation can be modified to permit its variation with the relaxation time. Furthermore, since the temperature dependence of the relaxation time on $1/T$ is in many cases non-linear and can be fairly well expressed as function of $(1/T)^\alpha$ [7], the relation (12) can be written in a more general form

$$\ln \lambda = \ln \kappa + U(\ln \kappa)F(T, T_R). \tag{13}$$

The Williams, Landel, Ferry relation expresses the dependence of the logarithm of the ratio of all mechanical and electrical relaxation times at temperature T to their values at a reference temperature T_R. In the notation used it can be written as

$$\ln \frac{\lambda}{\kappa} = \ln a_T = -\frac{C_1(T - T_R)}{C_2 + T - T_R}. \tag{14}$$

Although these authors in comparing their formula with other time–temperature relations, related it also to the viscosity-free volume relation of Doolittle [8], the comparison here is made with the free volume concept as modified by Turnbull and Cohen [9]. In this concept the free volume is related to the two regimes of the thermal expansion of the amorphous phase and thus the viscosity-free volume relation is replaced by a viscosity–temperature relation.

In molecularly simple substances the transition from liquid to glass is manifested by marked changes in viscosity, specific heat, and thermal expansion coefficient within a narrow temperature interval centering about a glass temperature T_g. The dependence of the specific volume on temperature is shown schematically below.

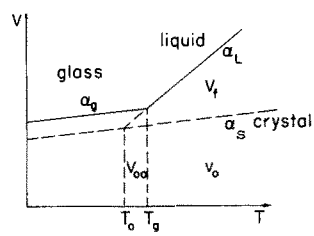

Specific volume–temperature relation.

The specific volume of the amorphous phase in the liquid and glassy state is shown by a solid line, and the dashed line shown corresponds to a hypothetical specific volume corresponding to the crystalline phase. Also shown are the corresponding coefficients of thermal expansion. The free volume V_f is specified as the difference, between the specific volume V and the occupied volume V_0, corresponding to the crystalline phase. For temperature $T > T_g$ the respective volumes are:

$$V = V_{00} + \alpha_L(T - T_0),$$
$$V_0 = V_{00} + \alpha_S(T - T_0),$$
$$V_f = V - V_0 = (\alpha_L - \alpha_S)(T - T_0).$$

Substitution into the Doolittle formula $\eta = A \exp(BV_0/V_f)$ leads to

$$\ln \eta = \ln A + B\frac{\alpha_S}{\alpha_L - \alpha_S} + B\frac{V_{00}}{\alpha_L - \alpha_S}\frac{1}{T - T_0}. \tag{15}$$

The logarithm of the ratio of η at temperature T and at a reference temperature T_R is easily evaluated and can be written as

$$\ln \frac{\lambda}{\kappa} = \ln a_T = \ln \frac{\eta_T}{\eta_{T_R}} = -\frac{BV_{00}}{\alpha_L - \alpha_S}\frac{1}{T_R - T_0}\frac{T - T_R}{T - T_R + (T_R - T_0)}. \tag{16}$$

Equation (16) is equivalent to equation (14) with

$$C_1 = \frac{BV_{00}}{\alpha_L - \alpha_S}\frac{1}{T_R - T_0}$$

and $C_2 = T_R - T_0$.

Equation (15) shows that the logarithm of viscosity depends linearly on $1/T - T_0$. However, the temperature T_0 is not known before hand for any system and has to be found by trial and error. Miller [10] has investigated the data of Fox and Flory on viscosity of polystyrene and polyisobutylene fraction and found that the constant $BV_{00}/\alpha_L - \alpha_S$ depends on the molecular weight, increasing with molecular weight for low molecular weights and approaching a constant for large molecular weights.

If this variation is attributed to the length of the molecular chains or segments in motion due to the applied stress or strain, then the behavior of any system must reflect the distribution of chains lengths or segments in a distribution of time–temperature dependences. Equation (16) should then indicate this variation by replacing the constant $BV_{00}/\alpha_L - \alpha_S$ by a function of $\ln \kappa$ and thus this can be written as

$$\ln \lambda = \ln \kappa + U(\ln \kappa)F(T, T_R) \tag{17}$$

which is the same as equation (13).

If we now denote the intensity of the spectrum of relaxation times at the reference temperature T_R by $H_1(\ln \kappa) = dG/d \ln \kappa$ and at the temperature T by $H_2(\ln \lambda) = dG/d \ln \lambda$, these two can be compared at T_R if $H_2(\ln \lambda)$ is "reduced" in the usual way; thus

$$H_1(\ln \kappa) = \frac{dG}{d \ln \kappa} = \frac{d_R T_R}{dT}\frac{dG}{d \ln \lambda}\frac{d \ln \lambda}{d \ln \kappa} = \frac{d_R T_R}{dT}H_2(\ln \lambda)\left\{1 + \frac{dU(\ln \kappa)}{d \ln \kappa}F(T, T_R)\right\} \tag{18}$$

where d_R is the density at T_R, d the density at T, and $\mathrm{d}\ln\lambda/\mathrm{d}\ln\kappa$ is evaluated from equation (17). Equation (18) can be rewritten as

$$H_2(\ln\lambda) = \frac{H_1(\ln\kappa)}{1+[\mathrm{d}U(\ln\kappa)/\mathrm{d}\ln\kappa]F(T, T_R)} \frac{dT}{d_R T_R}. \tag{19}$$

This equation shows that the temperature change from T_R to T is equivalent not only to a shift of the spectrum as determined by equation (17) but also the intensity of the spectrum is doubly affected. The first influence accounts for the proportionality of the moduli to absolute temperature while the second, responsible for the change of shape, is a measure of the variation of the rate at which the different portions of the spectrum shift with change of temperature.

5. EVALUATION OF EXPERIMENTAL RESULTS

In the evaluation of the experimental results shown in Fig. 8, the curves showing the dependence of the storage modulus on log $1/\omega$ at the various test temperatures were first reduced to the reference temperature and drawn on a common time scale. From horizontal lines drawn at arbitrarily chosen values of $G'(\omega)$ the shift factors corresponding to the various temperature changes were determined, and the product $U(\ln\kappa)\ F(T, T_R)$ evaluated. If the experimental data were sufficiently extensive both functions could be determined; however, in this case, because of the limited coverage, the temperature dependence was assumed to be linear with $1/T$ and equation (13) with $F(T, T_R) = (1/T - 1/T_R)$ was used. The function $U(\ln\kappa)$ was then readily evaluated and the portions of the spectra corresponding to the various $G'(\omega)$ curves determined by equation (11). As these portions of the spectra were derived from data already reduced, they were shifted into proper positions in accordance with equation (16), but omitting the reduction factor dT/d_0T_0.

From the spectrum thus derived both the storage modulus and the loss modulus, as well as the relaxation modulus, were recomputed and are shown with the spectrum in Fig. 9.

The extension of the time scale is relatively modest but the agreement with test results obtained in another investigation appears to be rather good. The test results shown as dots in the ranges of 10^{-2} to 10^{-3} sec were obtained from free vibrations of sandwich shear beams, those around 1 sec are from torsion pendulum measurements, and the open circles are relaxation measurements obtained previously.

6. SECOND-ORDER EFFECTS

Torsion of wires, circular bars or tubes appears to be the most suitable method for the study of second order or "cross" effects in solid or pseudo-solid materials as the torsion induced changes of length, or the rise of normal forces necessary to maintain the specimens at constant length can be observed as a separate phenomenon.

The second-order effects in liquids have been extensively studied and there is a substantial literature on this subject [11], in solids these studies were limited to the elastic range so far and very little is known about such effects in visco-elastic materials.

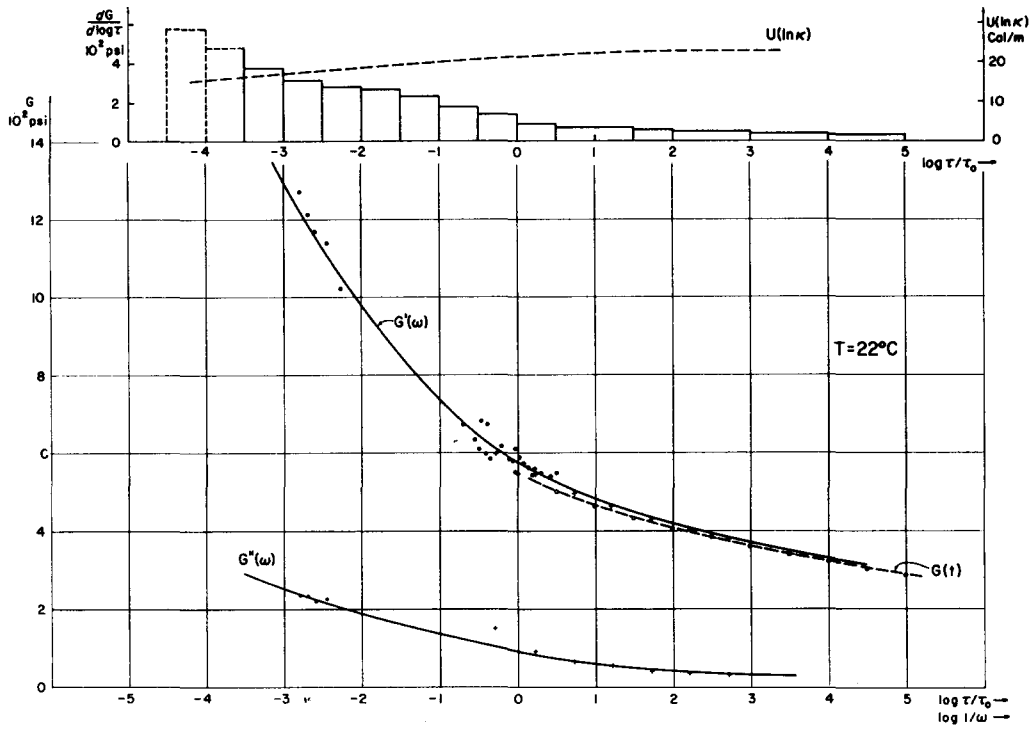

FIG. 9. Spectrum of relaxation times derived from the experimental results and the computed storage and loss moduli.

Second-order phenomena may be the result of nonlinearity of the strain–displacement relations, termed "geometric nonlinearity" or the result of nonlinearity of the constitutive tensor relations, termed "tensorial nonlinearity" [12]. In the first case the second-order effects are governed by the parameters of the first-order phenomena, while in the second case, the phenomena are governed by specific second-order material parameters which must be determined by suitable experiments.

The theory of second-order effects in isotropic incompressible elastic media due to nonlinearity of the strain–displacement relations was developed by Rivlin [13], while Reiner [14] formulated the tensorial relations for isotropic viscous fluids and isotropic elastic solids where the second order effects, the cross-viscosity and cross-elasticity are due to nonlinear tensorial relations. Reiner's concept of tensorial nonlinearity has been in turn applied to simple visco-elastic media by Rivlin and Ericksen [15]. The significance of the two approaches to second order phenomena is discussed in detail by Ronay and Freudenthal [12] and it is shown that while both the "geometric" and the "tensorial" nonlinearity contribute to the second order effects in solids, the "geometric" contribution can be neglected for small strains.

The Rivlin–Ericksen constitutive equation for a simple isotropic visco-elastic medium expresses the stress matrix $\tilde{T}$ as the sum of matrix polynomial in two kinematic matrices, the strain matrix $\tilde{E}$ and the deformation rate matrix $\tilde{D}$, and on the basis of a generalization of the Cayley–Hamilton theorem, this sum is reduced to the following form

$$\begin{aligned}\tilde{T} = {} & \alpha_0 \tilde{T} + \alpha_1 \tilde{E} + \alpha_2 \tilde{E}^2 + \alpha_3 \tilde{D} + \alpha_4 \tilde{D}^2 \\ & + \alpha_5[\tilde{E}\tilde{D} + \tilde{D}\tilde{E}] + \alpha_6[\tilde{E}^2\tilde{D} + \tilde{D}\tilde{E}^2] \\ & + \alpha_7[\tilde{E}\tilde{D}^2 + \tilde{D}^2\tilde{E}] + \alpha_8[\tilde{E}^2\tilde{D}^2 + \tilde{D}^2\tilde{E}^2]\end{aligned} \tag{20}$$

where the α_i are polynomials in the invariants of the matrices appearing in this equation. For small strains equation (20) can be written in tensorial form as

$$\begin{aligned}\sigma_{ij} = {} & \alpha_0\delta_{ij} + \alpha_1\varepsilon_{ij} + \alpha_2\varepsilon_{ik}\varepsilon_{kj} + \alpha_3\dot{\varepsilon}_{ij} + \alpha_4\dot{\varepsilon}_{ik}\dot{\varepsilon}_{kj} \\ & + \alpha_5[\varepsilon_{ik}\dot{\varepsilon}_{kj} + \dot{\varepsilon}_{ik}\varepsilon_{kj}] + \alpha_6[\varepsilon_{ik}\varepsilon_{kl}\dot{\varepsilon}_{lj} + \dot{\varepsilon}_{ik}\varepsilon_{kl}\varepsilon_{lj}] \\ & + \alpha_7[\varepsilon_{ik}\dot{\varepsilon}_{kl}\dot{\varepsilon}_{lj} + \dot{\varepsilon}_{ik}\dot{\varepsilon}_{kl}\varepsilon_{lj}] + \alpha_8[\varepsilon_{ik}\varepsilon_{kl}\dot{\varepsilon}_{lm}\dot{\varepsilon}_{mj} + \dot{\varepsilon}_{ik}\dot{\varepsilon}_{kl}\varepsilon_{lm}\varepsilon_{mj}].\end{aligned} \tag{21}$$

The nine coefficients in equation (21) can, in principle, be determined by experimental methods, but the difficulties increase with the degree of the terms involved as each successive power decreases the order of the measured quantities. Thus it is reasonable to reduce equation (21) to first- and second-degree terms only by setting $\alpha_6 = \alpha_7 = \alpha_8 = 0$. With this limitation and the introduction of the incompressibility condition equation (21) can be rewritten as

$$\begin{aligned}s_{ij} = {} & \alpha_1 e_{ij} + \alpha_3 \dot{e}_{ij} \\ & + \alpha_2\left(e_{ik}e_{kj} - \delta_{ij}\frac{\varepsilon_{\alpha k}\varepsilon_{k\alpha}}{3}\right) + \alpha_4\left(\dot{e}_{ik}\dot{e}_{kj} - \delta_{ij}\frac{\dot{\varepsilon}_{\alpha k}\dot{\varepsilon}_{k\alpha}}{3}\right) \\ & + \alpha_5\left(e_{ik}\dot{e}_{kj} - \delta_{ij}\frac{\varepsilon_{\alpha k}\dot{\varepsilon}_{k\alpha}}{3} + \dot{e}_{ik}e_{kj} - \delta_{ij}\frac{\dot{\varepsilon}_{\alpha k}\varepsilon_{k\alpha}}{3}\right)\end{aligned} \tag{22}$$

where

$$s_{ij} = \sigma_{ij} - \delta_{ij}\frac{\sigma_{\alpha\alpha}}{3} \quad \text{and} \quad e_{ij} = \varepsilon_{ij} - \delta_{ij}\frac{\varepsilon_{\alpha\alpha}}{3}.$$

In this equation the coefficients α_2, α_4 and α_5 are the second-order material parameters, and if they are zero equation (22) reduces to the constitutive equation of a linear incompressible Kelvin body. It is worth noting that if shear strain ε_{MN}, $M \neq N$, is imposed, there will be no contribution to σ_{MN} from the second-order terms, while σ_{MM} and σ_{NN} will have contributions from the second order terms only. On the other hand, if uniaxial strain ε_{MM} is imposed, the contributions from the second order terms for small strain will hardly be measurable in relation to the primary effects.

Denoting the shear strain imposed by the Rheogoniometer $\varepsilon_{12} = \frac{1}{2}\gamma_0 \sin \omega t$ and the corresponding shear stress rate $\dot{\varepsilon}_{12} = \frac{1}{2}\gamma_0\omega \cos \omega t$, the normal stress σ_{11} is

$$\sigma_{11} = \frac{\alpha_2}{4}\gamma_0^2 \sin^2\omega t + \frac{\alpha_4}{4}\omega^2\gamma_0^2 \cos^2\omega t + \frac{2\alpha_5}{4}\omega\gamma_0^2 \sin \omega t \cos \omega t \tag{23}$$

where $\alpha_2/4$, $\alpha_4\omega^2/4$ and $2\alpha_5\omega/4$ are the cross-elasticity, cross-viscosity, and cross-elasticity-viscosity moduli respectively. Equation (23) can be rewritten as

$$\sigma_{11} = \frac{1}{2}\gamma_0^2\left\{\frac{\alpha_2}{4}(1 - \cos 2\omega t) + \frac{\alpha_4\omega^2}{4}(1 + \cos 2\omega t) + \frac{2\alpha_5\omega}{4}\sin 2\omega t\right\} \tag{23a}$$

showing that circular frequency of all the components of normal stress is double the frequency of the imposed shear strain. It also shows that the amplitude of the normal stress varies with the square of the amplitude of the imposed shear strain. The recorded stress–strain diagrams shown in Fig. 6 clearly show this behavior. In Fig. 10, the normal

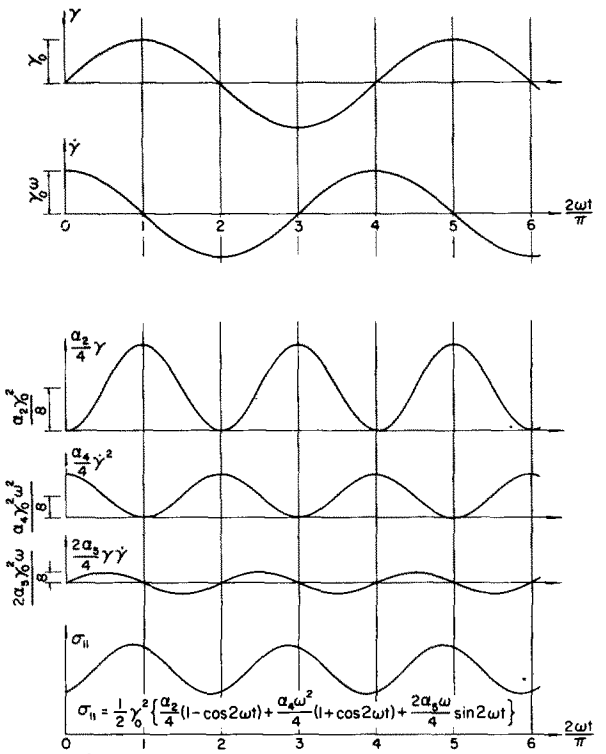

FIG. 10. Components of second order normal stress in tubular specimen in cyclical torsion imposing shear strain $\gamma = \gamma_0 \sin \omega t$.

stress σ_{11} and its three components as expressed by equation (23a) are shown as functions of $2\omega t/\pi$. For ease of presentation it was assumed that: $\alpha_4\omega^2 = \alpha_2/2$ and $2\alpha_5\omega = \alpha_2/4$. The corresponding stress–strain diagrams together with the primary effects are shown in Fig. 11.

Although all the recorded experimental stress–strain diagrams show the presence of all three components of the normal thrust, only the first two are sufficiently reliable for evaluation, and the evaluated cross-elasticity modulus $\alpha_2/4 = G_c'$ and the cross-viscosity modulus $\alpha_4\omega^2/4 = G_c''$ are shown as functions of $\log 1/\omega$ in Fig. 12. Both moduli G_c' and G_c'' are frequency and temperature dependent and probably could be characterized by continuous spectra; however the experimental results accumulated so far are limited and are insufficient for such characterization.

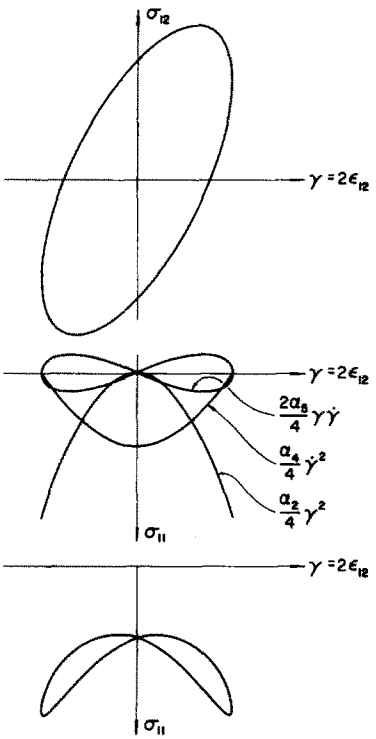

FIG. 11. Typical shear stress–strain and normal stress–shear strain diagrams in reversed torsion.

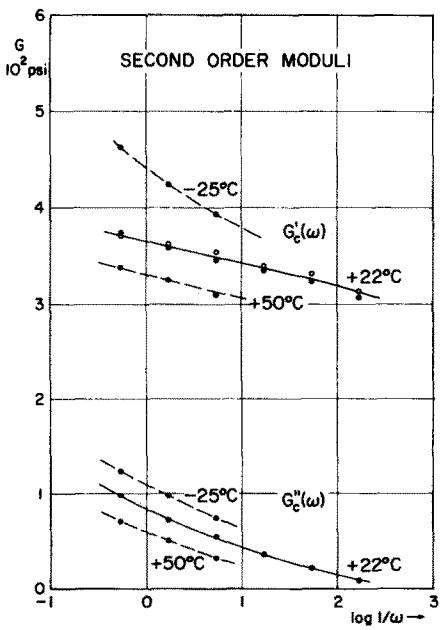

FIG. 12. Experimental values of second-order moduli.

REFERENCES

[1] E. M. LENOE, R. A. HELLER and A. M. FREUDENTHAL, *Trans. Soc. Rheol.* **9**, 77 (1965).
[2] F. R. EIRICH (ed.), *Rheology*, Vol. II, p. 503. Academic Press (1958).
[3] F. R. EIRICH (ed.), *Rheology*, Vol. II, p. 46. Academic Press (1958).
[4] H. LEADERMAN, *Elastic and Creep Properties of Filamentous Materials and Other High Polymers*, p. 77. The Textile Foundation, Washington, D.C. (1943).
[5] M. L. WILLIAMS, R. F. LANDEL and J. D. FERRY, *J. Am. Chem. Soc.* **77**, 3701 (1951).
[6] B. ALBRECHT, *J. appl. Phys.* **33**, 755 (1962).
[7] H. LEADERMAN and R. G. SMITH, *Phys. Rev.* **81**, 303 (1951);
T. G. FOX, Jr. and P. J. FLORY, *J. appl. Phys.* **21**, 581 (1950);
H. LEADERMAN, *J. Polym. Sci.* **13**, 371 (1954).
[8] A. K. DOOLITTLE, *J. appl. Phys.* **22**, 1471 (1951).
[9] D. TURNBULL and M. H. COHEN, *J. Chem. Phys.* **34**, 120 (1961).
[10] A. A. MILLER, *J. Polym. Sci.* **A1**, 1857 & 1865 (1963).
[11] A. S. LODGE, *Elastic Fluids*. Academic Press (1964).
[12] M. RONAY and A. M. FREUDENTHAL, *Proc. R. Soc.* A 1966 (in press).
[13] R. S. RIVLIN, *Phil. Trans. R. Soc.* A**240**, 459 (1948); **241**, 379 (1948); **242**, 173 (1949).
[14] M. REINER, *Am. J. Math.* **67**, 350 (1945); **70**, 433 (1948).
[15] R. S. RIVLIN and J. L. ERICKSEN, *J. ration. Mech. Analysis* **4**, 323 (1955).

(*Received* 20 *September* 1965)

Résumé—Le comportement mécanique du caoutchouc polyurethane empli de chlorure de potassium granulaire a été investigué en faisant subir à des specimens tubulaires une torsion oscillatoire. La réaction du materiel a été étudiée à des variations de fréquences et d'amplitude de la contrainte imposée aussi bien qu'à des variations de température.

A part le mesurage de l'emmagasinement et la perte de modules, les forces normales sont observées, et les modules de second ordre d'élasticité transversale, de viscosité transversale et de visco-élasticité transversale sont évaluées.

Zusammenfassung—Das mechanische Verhalten von Kunststoff Gummi, gefüllt mit Kaliumchlorid wurde untersucht bei Unterwerfung von röhrenförmigen Proben zu Schwingungsdrehungen. Die Empfänglichkeit des Materials für Frequenzen und Schwingungsveränderungen der auferlegten Beanspruchung, wie auch für Temperaturveränderungen wurde untersucht. Ausser den Messungen der Speicherung und von dem Verlust Modul, die normalen Kräfte wurden beobachtet und das Modul zweiter Ordnung von Querelastizität, Querviskosität und Querfliessverhalten wurde bewertet.

Абстракт—Механическое поведение полиуретановой резины, наполненной гранулированным хлористым калием исследовалось подверганием цилиндрических образцов колебательному кручению. Изучалось реагирование материала на изменения частоты и амплитуды приложенного напряжения-деформации, также, как на изменение температуры.

Кроме измерения модулей накопления и потери наблюдались нормальные силы и вычислены модули второго порядка—поперечной упругости, поперечной вязкости и поперечной вязкозластичности.